

## **RIGOROUS ANALYSIS OF RECTANGULAR WAVEGUIDE JUNCTIONS BY FOURIER TRANSFORM TECHNIQUE**

H. Jia, K. Yoshitomi, and K. Yasumoto

Department of Computer Science and Communication Engineering  
Kyushu University 36, Fukuoka 812-8581, Japan

- 1. Introduction**
- 2. Formulation of the Problem**
  - 2.1 E-plane Asymmetric T-junction
  - 2.2 H-plane T-junction
- 3. Numerical Examples**
- 4. Conclusion**

### **References**

### **1. INTRODUCTION**

Rectangular waveguides with various kinds of discontinuity are widely used in the design of microwave components, such as multiplexers, power dividers, and filters in modern communication systems. The accurate analysis of waveguide discontinuities has been one of important subjects to establish the design method for several decades. A variety of purely numerical techniques or analytical and numerical approaches have been developed for analyzing the bends and T-junctions in rectangular waveguides. The finite element method [1], the boundary element method [2], and the method of lines [3, 4] are versatile numerical techniques and have been successfully applied to solve the H-plane or E-plane discontinuities. However these methods require considerable computational effort.

The mode-matching method is typical of analytical and numerical approaches. A wide range of waveguide discontinuities has a configuration in which several uniform waveguide sections are connected through a cavity region. The mode-matching method uses the expansions of

the fields in the waveguide sections in terms of their normal modes. The expanded fields are matched to those of the cavity region to obtain the modal scattering matrix of the discontinuity. This requires a resonant mode expansion of the cavity fields [5, 6] or the use of dyadic Green's function in the cavity region [7]. In order to avoid such a sophisticated field analysis of the cavity, various techniques [8, 13] based on equivalent circuit concepts have been incorporated in the mode-matching procedure. The cavity problem with multiapertures can be reduced [8] to a superposition of simpler cavity problems by subsequently shorting all apertures but one, to which the field expansions by the normal modes can be applied. This principle has been used to analyze asymmetric series E-plane T-junctions [9] and generalized rectangular aperture-coupled T-junctions [10]. The three plane mode-matching technique [11] has been presented for characterizing symmetric E- and H-plane T-junctions. This technique reduces the problem of T-junctions to a waveguide discontinuity problem of three waveguides, and the scattering matrix of the original T-junction can be calculated by analyzing the discontinuity problem three times with different positions of the short circuit on the side arm. Recently this approach has been extended to the port reflection coefficient method [12] for multiport waveguide junctions. A mode-matching technique [13] similar to [8] has been developed to obtain the generalized admittance matrix in closed form for three- and four-port waveguide junctions. The mode-matching method combined with the equivalent-circuit concepts [8–13] provides a rigorous and efficient technique for analyzing rectangular waveguide junctions, without using the dyadic Green's function in the cavity region. However the method requires that the reduced waveguide structures with the short circuit in different positions be repeatedly treated.

In this paper, we present the mode-matching method combined with the Fourier transform technique for analyzing rigorously rectangular waveguide junctions. In this method, the fields of the main waveguide represented by the Fourier integral are matched to those of the side arm expressed in term of an infinite set of normal modes. The mode-matching process in the spatial domain has been discussed [14] for the E-plane T-junction to derive a singular integral equation for the aperture field, which leads the variational form for the equivalent circuit parameters. When the mode-matching is performed in the Fourier transformed domain, on the other hand, a set of linear alge-

braic equations for the field expansion coefficients is obtained, from which the circuits parameters are numerically determined. Recently this approach has been successfully applied to the aperture problems [15, 16] in parallel-plate waveguides and a problem of open junctions [17] in a rectangular waveguide. However one notes a difficulty in applying the approach to general configurations of waveguide junction in which there is no uniform waveguide section of infinite extent. Here the image theory based on the equivalence principle is adopted. We introduce an image waveguide to the side-arm of the junction and transform the original problem into an aperture problem in a uniform rectangular waveguide of infinite extent. Then the fields in the cavity region are expressed by Fourier integrals, which can be evaluated in closed form by a simple residue-calculus. The fields are matched to those of other arms expanded by the respective normal modes. This yields a system of linear equations to determine the scattering parameters of the junction. The main advantage of the method is that the scattering parameters are calculated at one time by solving matrix equations of relatively small dimensions, without repeating the analyses for the reduced waveguide structures with several short circuit conditions.

The proposed method is applied to the analyses of right-angle corner bends in rectangular waveguides, symmetric E- and H-plane T-junctions, asymmetric E- and H-plane T-junctions, and asymmetric series E-plane T-junctions. It is shown that the convergence of our numerical solutions is very fast. The results are compared with available numerical and experimental data [2, 4, 6, 9, 11]. The good agreement between them confirms the validity of the present method.

## 2. FORMULATION OF THE PROBLEM

Figure 1(a) shows a cross sectional view in the  $y-z$  plane of an asymmetric T-junction, which consists of three rectangular waveguides  $I$ ,  $II$ , and  $III$ . The cross sectional dimensions of three waveguides are  $2a \times 2w_I$ ,  $2a \times 2w_{II}$ , and  $2a \times 2b$  in the  $x-y$  plane, respectively. The left side end of semi-infinite waveguide  $III$  is short-circuited at  $y = 0$ . This junction represents a E-plane T-junction when  $a > b$  and a H-plane T-junction when  $a < b$ . In order to apply the Fourier transform technique to the fields in the semi-infinite waveguide  $III$ , we introduce an image waveguide structure in  $y < 0$ . Figure 1(b) shows the whole waveguide structure constituted from the original waveguides in  $y > 0$  and the image waveguides in  $y < 0$ . The configuration is symmetric

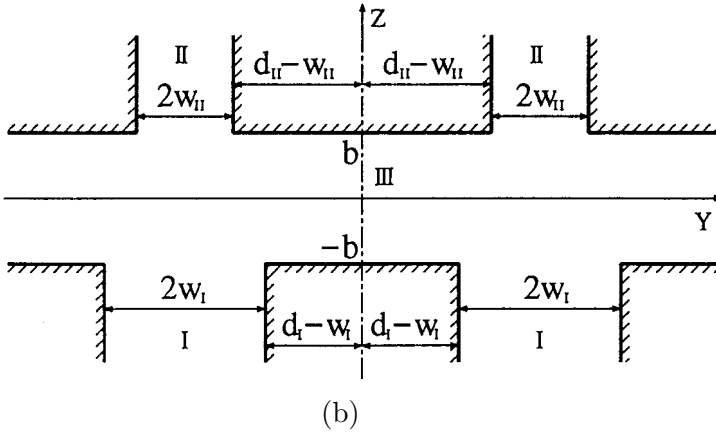
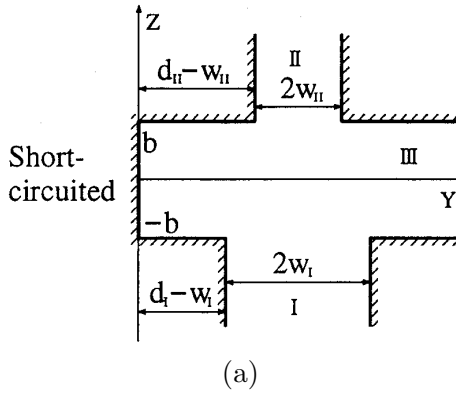


**Figure 1.** Longitudinal cross section of an asymmetric T-junction; (a) original T-junction and (b) equivalent structure with image waveguides.

with respect to  $y = 0$ . The electric and magnetic fields in  $y < 0$  are defined through the following relations of symmetry:

$$\hat{y} \times \mathbf{E}_\nu(x, -y, z) = -\hat{y} \times \mathbf{E}_\nu(x, y, z) \tag{1}$$

$$\hat{y} \times \mathbf{H}_\nu(x, -y, z) = \hat{y} \times \mathbf{H}_\nu(x, y, z) \quad \text{for } \nu = I, II, III. \tag{2}$$

By introducing the image waveguides, the semi-infinite waveguide III was transformed into an infinite uniform waveguide to which we can apply the Fourier transform technique.

### 2.1 E-plane Asymmetric T-junction

We discuss first the case of E-plane T-junction with  $a > b$ . For the analysis of series T-junctions discussed later, we consider a general situation in which both  $TE_{1m}$  and  $TM_{1m}$  modes are incident in the waveguides  $I$  and  $II$ . Since the E-plane T-junction has the common dimension  $2a$  in the  $x$  direction, the fields scattered into waveguides  $I$ ,  $II$ , and  $III$  have the same  $x$  dependence as the incident waves. We use the field representation by the longitudinal section  $TE_{1m}^x$  waves [9]. Then the incident and scattered waves in waveguides  $I$  and  $II$  are expressed by the magnetic Hertzian vectors as follows:

$$\begin{aligned} \mathbf{\Pi}_\nu &= \frac{\hat{x}}{k_0^2 Z_0} \sin \left[ \frac{\pi}{2a}(x+a) \right] \sum_{m=0}^{\infty} \left[ A_{\nu m} e^{\mp j\beta_{\nu m}^e(z \pm b)} + B_{\nu m} e^{\pm j\beta_{\nu m}^e(z \pm b)} \right] \\ &\quad \times \cos [\xi_{\nu m}(y - d_\nu + w_\nu)] \quad \text{for } \nu = I, II \end{aligned} \tag{3}$$

where  $\beta_{\nu m}^e = \sqrt{k_0^2 - (\pi/2a)^2 - \xi_{\nu m}^2}$ ,  $\xi_{\nu m} = m\pi/2w_\nu$ ,  $k_0 = \omega\sqrt{\epsilon_0\mu_0}$  and  $Z_0 = \sqrt{\mu_0/\epsilon_0}$  are the wave number and intrinsic impedance in free space,  $A_{\nu m}$  are the amplitudes of incident  $TE_{1m}^x$  modes in waveguide  $\nu$ , and  $B_{\nu m}$  are unknown expansion coefficients for scattered waves. The upper (lower) sign in exponential functions corresponds to  $\nu = I$  ( $\nu = II$ ). Note that the electric fields derived from the Hertzian vectors (3) satisfy the boundary conditions on the conducting walls at  $x = \pm a$  and  $y = d_\nu \pm w_\nu$ .

The Fourier transform technique is used to represent the transmitted fields in waveguide  $III$  on the basis of discussion in the preceding subsection. The magnetic Hertzian vector in waveguide  $III$  are then expressed by using the Fourier integrals as follows:

$$\begin{aligned} \mathbf{\Pi}_{III} &= \frac{\hat{x}}{2\pi k_0^2 Z_0} \sin \left[ \frac{\pi}{2a}(x+a) \right] \\ &\quad \times \int_{-\infty}^{\infty} \{ A(\eta) \cos [\gamma_e(z+b)] + B(\eta) \cos [\gamma_e(z-b)] \} e^{-j\eta y} d\eta \end{aligned} \tag{4}$$

where  $\gamma_e = \sqrt{k_0^2 - (\pi/2a)^2 - \eta^2}$ , and  $A(\eta)$  and  $B(\eta)$  are unknown spectral functions. The electric field derived from (4) satisfies the boundary conditions on the conducting walls at  $x = \pm a$ .

The tangential components of electric and magnetic fields derived from (3) and (4) should be continuous across the boundary planes

$z = \pm b$ . These boundary conditions may be expressed as

$$E_{IIIy}(x, y, \mp b) = \begin{cases} E_{\nu y}(x, y, \mp b) & |y - d_\nu| \leq w_\nu \\ E_{\nu y}(x, |y|, \mp b) & |y + d_\nu| \leq w_\nu \\ 0 & \text{otherwise} \end{cases} \quad (5)$$

$$H_{IIIx}(x, y, \mp b) = H_{\nu x}(x, y, \mp b) \quad |y - d_\nu| \leq w_\nu \quad \text{for } \nu = I, II. \quad (6)$$

The boundary conditions for the electric fields are first applied. The electric fields derived from (3) and (4) are substituted into (5), and Fourier transforms of the resulting expressions are calculated. This leads to a set of equations which relate the unknown spectral functions  $A(\eta)$  and  $B(\eta)$  to the expansion coefficients  $A_{\nu m}$  and  $B_{\nu m}$  as follows:

$$\begin{cases} A(\eta) = \frac{-1}{\gamma_e \sin(2\gamma_e b)} \sum_{m=0}^{\infty} \beta_{II m}^e (A_{II m} - B_{II m}) [C_{II m}(\eta) + C_{II m}(-\eta)] \\ B(\eta) = \frac{-1}{\gamma_e \sin(2\gamma_e b)} \sum_{m=0}^{\infty} \beta_{I m}^e (A_{I m} - B_{I m}) [C_{I m}(\eta) + C_{I m}(-\eta)] \end{cases} \quad (7)$$

where

$$C_{\nu m}(\eta) = \frac{\eta e^{j\eta d_\nu}}{\eta^2 - \xi_{\nu m}^2} [(-1)^m e^{j\eta w_\nu} - e^{-j\eta w_\nu}] \quad (8)$$

Using (7) in (4), the Hertzian vectors in waveguide III and hence the magnetic fields  $H_{IIIx}(x, y, \mp b)$  are expressed in terms of the expansion coefficients  $A_{\nu m}$  and  $B_{\nu m}$ . The results are substituted into the boundary conditions (6) for the magnetic fields together with the corresponding expressions of  $H_{\nu x}(x, y, \mp b)$  ( $\nu = I, II$ ) derived from (3). Then we integrate (6) from  $y = d_\nu - w_\nu$  to  $y = d_\nu + w_\nu$  after multiplying both sides by the trigonometric functions  $\cos[\xi_{\nu n}(y - d_\nu + w_\nu)]$ , where  $n$  is nonnegative integers. This leads to a set of linear equations for the expansion coefficients  $A_{\nu m}$  and  $B_{\nu m}$  as follows:

$$\begin{aligned} & -j [A_{In} + B_{In}] w_I (\delta_{n0} + 1) \\ & = \sum_{m=0}^{\infty} \beta_{Im}^e (A_{Im} - B_{Im}) F_I + \sum_{m=0}^{\infty} \beta_{II m}^e (A_{II m} - B_{II m}) G_{II}^I \end{aligned} \quad (9)$$

$$\begin{aligned} & -j [A_{II n} + B_{II n}] w_{II} (\delta_{n0} + 1) \\ & = \sum_{m=0}^{\infty} \beta_{Im}^e (A_{Im} - B_{Im}) G_I^{II} + \sum_{m=0}^{\infty} \beta_{II m}^e (A_{II m} - B_{II m}) F_{II} \end{aligned} \quad (10)$$

for  $n = 0, 1, 2, \dots$

where

$$F_\nu = \frac{1}{2\pi} \int_{-\infty}^{\infty} \frac{C_{\nu n}(-\eta)}{\gamma_e \tan(2\gamma_e b)} [C_{\nu m}(\eta) + C_{\nu m}(-\eta)] d\eta \tag{11}$$

$$G_\nu^\mu = \frac{1}{2\pi} \int_{-\infty}^{\infty} \frac{C_{\mu n}(-\eta)}{\gamma_e \sin(2\gamma_e b)} [C_{\nu m}(\eta) + C_{\nu m}(-\eta)] d\eta \tag{12}$$

for  $\nu, \mu = I, II$ .

The integrals in (11) and (12) can be evaluated in closed form by a simple residue-calculus. For example, we have

$$F_I = \frac{-w_I(1 + \delta_{n0})\delta_{mn}}{\gamma_e \tan(2\gamma_e b)|_{\eta=\xi_{Im}}} - \sum_{p=0}^{\infty} \frac{j\eta_p [1 - (-1)^m e^{-2j\eta_p w_I}] Q_{mn}}{b(1 + \delta_{p0})(\eta_p^2 - \xi_{In}^2)(\eta_p^2 - \xi_{Im}^2)}$$

$$j\eta_p \left\{ [(-1)^m + (-1)^n] e^{-2j\eta_p d_I} - (-1)^{m+n} e^{-2j\eta_p(d_I+w_I)} - e^{-2j\eta_p(d_I-w_I)} \right\}$$

$$- \sum_{p=0}^{\infty} \frac{\quad}{2b(1 + \delta_{p0})(\eta_p^2 - \xi_{In}^2)(\eta_p^2 - \xi_{Im}^2)} \tag{13}$$

with

$$Q_{mn} = \begin{cases} 1 & m + n \stackrel{\Delta}{=} \text{even} \\ 0 & m + n \stackrel{\Delta}{=} \text{odd} \end{cases} \tag{14}$$

where  $\eta_p = \sqrt{k_0^2 - (\pi/2a)^2 - (p\pi/2b)^2}$ , and  $\delta_{mn}$  denotes the Kronecker delta. Although other details have been omitted,  $F_\nu$  and  $G_\nu^\mu$  are given in terms of the series with very fast convergence in proportion to  $\eta_p^{-3}$ . When the excitation condition is given, the amplitudes  $A_{\nu m}$  of incident  $TE_{1m}^x$  modes into waveguide  $\nu$  are specified. Then (9) and (10) are solved to obtain the unknown expansion coefficients  $B_{\nu m}$  for the scattered waves into waveguides  $I$  and  $II$ , after truncating the modal expansion up to  $m = M$ . The results are used in (7) to determine the unknown spectral functions  $A(\eta)$  and  $B(\eta)$ . When the T-junction in Fig. 1 (a) with  $a > b$  is excited by  $TE_{10}$  mode incident from waveguide  $I$ , we have  $A_{Im} = 0$  for  $m > 0$  and  $A_{II m} = 0$  for  $m \geq 0$ . For this excitation, the scattering parameters are calculated in terms of expansion coefficients rooted by (9) and (10) with (7) as

follows:

$$s_{11} = \frac{B_{I0}}{A_{I0}} \quad (15)$$

$$s_{21} = \frac{B_{II0}}{A_{I0}} \sqrt{\frac{w_{II}}{w_I}} \quad (16)$$

$$s_{31} = \frac{-j\sqrt{b/w_I}}{4b\eta_0 A_{I0}} \left\{ \sum_{m=0}^M \beta_{Im}^e (A_{Im} - B_{Im}) [C_{Im}(\eta_0) + C_{Im}(-\eta_0)] \right. \\ \left. + \sum_{m=0}^M \beta_{II m}^e (A_{II m} - B_{II m}) [C_{II m}(\eta_0) + C_{II m}(-\eta_0)] \right\} \quad (17)$$

The other elements of scattering matrix are obtained by changing the port of initial excitation.

The present Fourier transform technique is easily extended to two series T-junctions as shown in Fig. 2. Since waveguides  $II$  and  $I'$  are common to both T-junctions, we have

$$\mathbf{\Pi}_{II}(x, y, z) = \mathbf{\Pi}_{I'}(x', y', z') \quad (18)$$

$$\begin{cases} A_{II m} = B'_{Im} e^{-j\beta_{II m}^e h} \\ B_{II m} = A'_{Im} e^{j\beta_{II m}^e h} \end{cases} \quad (19)$$

Although the matrix size becomes a little larger, the solutions are obtained by connecting two systems of linear equations as (9) and (10) for each isolated single T-junction through the relations (19).

## 2.2 H-plane T-junction

When  $a < b$ , the junction shown in Fig. 1 represents a H-plane T-junction. In this case, we use the field representation in terms of  $TM^X$  waves. Let the  $TE_{01}$  mode with the amplitude  $A_0$  be incident from  $z = -\infty$  in waveguide  $I$ . Then the incident and scattered waves into waveguides  $I$ ,  $II$ , and  $III$  are expressed by the electric Hertzian vectors as follows:

$$\mathbf{\Pi}_I = \frac{\hat{x}}{k_0^2} \sum_{m=1}^{\infty} \sin[\xi_{Im}(y - d_I + w_I)] \left[ A_0 \delta_{m1} e^{-j\beta_{I1}^h(z+b)} + A_m e^{j\beta_{Im}^h(z+b)} \right] \quad (20)$$

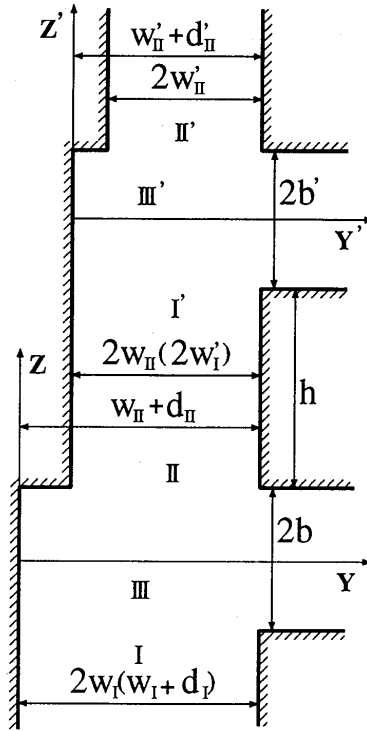


Figure 2. Longitudinal cross section of two series T-junctions.

$$\Pi_{II} = \frac{\hat{x}}{k_0^2} \sum_{m=1}^{\infty} \sin [\xi_{II m}(y - d_{II} + w_{II})] B_m e^{-j\beta_{II m}^h(z-b)} \quad (21)$$

$$\Pi_{III} = \frac{\hat{x}}{2\pi k_0^2} \int_{-\infty}^{\infty} \{C(\eta) \sin \gamma_h(z + b) + D(\eta) \sin \gamma_h(z - b)\} e^{-j\eta y} d\eta \quad (22)$$

where  $\beta_{\nu m}^h = \sqrt{k_0^2 - \xi_{\nu m}^2}$ , ( $\xi_{\nu m} = m\pi/2w_{\nu}$ ) ( $\nu = I, II$ ),  $\gamma_h = \sqrt{k_0^2 - \eta^2}$ ,  $A_m$  and  $B_m$  are unknown expansion coefficients, and  $C(\eta)$  and  $D(\eta)$  are unknown spectral functions. Following the similar analytical technique to the E-plane case, we have the following relations:

$$\begin{cases} C(\eta) = \frac{1}{\sin 2\gamma_h b} \sum_{m=1}^{\infty} B_m [S_{II m}(\eta) - S_{II m}(-\eta)] \\ D(\eta) = \frac{-1}{\sin 2\gamma_h b} \sum_{m=1}^{\infty} (A_0 \delta_{m1} + A_m) [S_{I m}(\eta) - S_{I m}(-\eta)] \end{cases} \quad (23)$$

where

$$S_{\nu m}(\eta) = \frac{\xi_{\nu m} e^{j\eta d_{\nu}}}{\eta^2 - \xi_{\nu m}^2} [(-1)^m e^{j\eta w_{\nu}} - e^{-j\eta w_{\nu}}]. \tag{24}$$

The linear equations to determine the unknown expansion coefficients  $A_m$  and  $B_m$  are also given by

$$jw_I \beta_{In}^h (A_0 \delta_{n1} - A_n) = \sum_{m=1}^{\infty} (A_0 \delta_{m1} + A_m) F_I - \sum_{m=1}^{\infty} B_m G_{II}^I \tag{25}$$

$$jw_{II} \beta_{II n}^h B_n = \sum_{m=1}^{\infty} (A_0 \delta_{m1} + A_m) G_I^{II} - \sum_{m=1}^{\infty} B_m F_{II} \tag{26}$$

for  $n = 1, 2, 3 \dots$

where

$$F_{\nu} = \frac{1}{2\pi} \int_{-\infty}^{\infty} \frac{k_0^2 - \eta^2}{\gamma_h \tan(2\gamma_h b)} [S_{\nu m}(\eta) - S_{\nu m}(-\eta)] S_{\nu n}(-\eta) d\eta \tag{27}$$

$$G_{\nu}^{\mu} = \frac{1}{2\pi} \int_{-\infty}^{\infty} \frac{k_0^2 - \eta^2}{\gamma_h \sin(2\gamma_h b)} [S_{\nu m}(\eta) - S_{\nu m}(-\eta)] S_{\mu n}(-\eta) d\eta \tag{28}$$

for  $\nu, \mu = I, II$ .

The integrals in (27) and (28) can be evaluated in closed form by a simple residue-calculus. Equations (25) and (26) are solved to obtain the unknown expansion coefficients  $A_m$  and  $B_m$ , after truncating the modal expansion up to  $m = M$ . The results are used in (23) to determine the unknown spectral functions  $C(\eta)$  and  $D(\eta)$ . Then the elements of the scattering matrix for the H-plane T-junction are given as follows:

$$s_{11} = \frac{A_1}{A_0} \tag{29}$$

$$s_{21} = \sqrt{\frac{w_I \beta_{II1}^h}{w_{II} \beta_{I1}^h}} \frac{B_1}{A_0} \tag{30}$$

$$s_{31} = \frac{\xi_{I1}}{4b\alpha A_0} \sqrt{\frac{w_I \alpha}{b \beta_{I1}^h}} \left\{ \sum_{m=1}^M B_m [S_{II m}(\alpha) - S_{II m}(-\alpha)] + \sum_{m=1}^M (A_0 \delta_{m1} + A_m) [S_{Im}(\alpha) - S_{Im}(-\alpha)] \right\} \tag{31}$$

where  $\alpha = \sqrt{k_0^2 - (\pi/2b)^2}$ .

### 3. NUMERICAL EXAMPLES

The proposed Fourier transform technique has been applied to various kinds of discontinuities in rectangular waveguides, and the results have been compared with those obtained by other numerical approaches. Although the present analysis is valid for any excitation, we assumed that the  $TE_{10}$  mode is incident from  $z < -b$  in waveguide  $I$  for the E-plane problem and the  $TE_{01}$  mode is incident for the H-plane problem. The scattering parameters were calculated from (15)–(17) and (29)–(31) for the respective cases. We considered first a right angle corner bend with  $w_{II} = d_{II} = 0$  and  $d_I = w_I$  in Fig. 1. The reflection coefficient  $|S_{11}|$  is plotted in Fig. 3 as functions of the normalized frequency  $f/f_c$  for the E-plane bend, where  $f_c$  is the cutoff frequency of  $TE_{10}$  mode in waveguide  $I$ . The marked values show the result obtained by the mode-matching method with the resonant mode expansion [6] for  $b/a = 0.5$ . Our result is in good agreement with that of the mode-matching method. It is seen that the return loss in the bend is significantly reduced with the decreasing  $b/a$ . Figure 4 shows the scattering parameter  $|S_{21}|^2$  for the H-plane bend as a function of the normalized frequency  $f/f_c$ , where  $f_c$  is the cutoff frequency of  $TE_{01}$  mode in waveguide  $I$ . In this case, the scattering parameters are independent of the waveguide dimension  $a$  in the  $x$  direction. The marked values show the result obtained by the boundary element method [2]. We can see a very close agreement in both results. Table I shows the convergence of the solutions versus the truncated number of modal expansion in waveguide  $I$ . When the mode number is truncated at  $M = 7$  ( $M = 3$ ) for E-plane (H-plane) bend, the errors in computation are achieved to be less than 0.1 %. The convergence is faster in the H-plane bend than in the E-plane bend. It is worth emphasizing that the results given in Table I satisfy accurately the relation  $|S_{11}|^2 + |S_{21}|^2 = 1$  for energy conservation.

When  $d_I = d_{II} = w_I = w_{II}$ , the waveguide junction in Fig. 1 is reduced to a symmetric T-junction. This symmetric configuration can be treated by the standard Fourier transform technique in the  $z$  direction along waveguides  $I$  and  $II$ . To verify the effectiveness of the proposed method, however, we applied the Fourier transform in the  $y$  direction to the field of waveguide  $III$  under the assumed

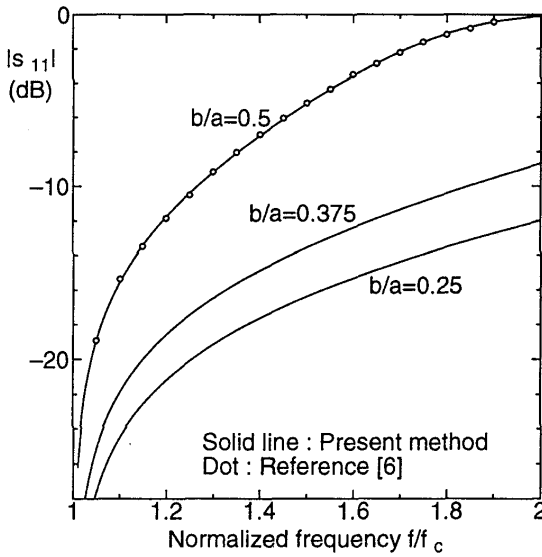


**Figure 3.** Reflection coefficient  $|S_{11}|$  as functions of frequency for E-plane right angle corner-bends with  $w_{II} = d_{II} = 0$  and  $d_I = w_I$  in Fig. 1.

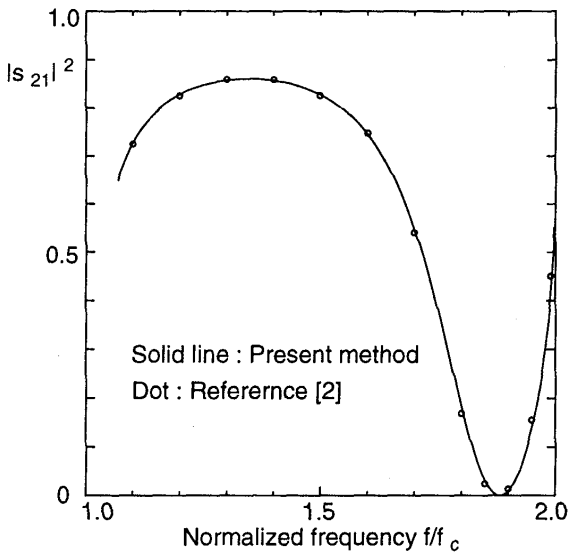


**Figure 4.** Power transmission coefficient  $|S_{21}|^2$  as a function of frequency for a H-plane right angle corner-bend.

| E-plane $b/a = 0.5$ $f/f_c = 1.5$ |                          |                         |
|-----------------------------------|--------------------------|-------------------------|
| M                                 | $S_{11}$                 | $S_{21}$                |
| 1                                 | 0.523109   $-2.22^\circ$ | 0.852265   $-0.8^\circ$ |
| 2                                 | 0.539847   $-5.89^\circ$ | 0.841763   $3.71^\circ$ |
| 3                                 | 0.544838   $-6.06^\circ$ | 0.838541   $4.20^\circ$ |
| 4                                 | 0.546877   $-6.07^\circ$ | 0.837213   $4.37^\circ$ |
| 5                                 | 0.547942   $-6.06^\circ$ | 0.836516   $4.45^\circ$ |
| 6                                 | 0.548582   $-6.05^\circ$ | 0.836097   $4.50^\circ$ |
| 7                                 | 0.549004   $-6.04^\circ$ | 0.835820   $4.53^\circ$ |
| 8                                 | 0.549300   $-6.03^\circ$ | 0.835625   $4.55^\circ$ |
| 9                                 | 0.549517   $-6.02^\circ$ | 0.835482   $4.57^\circ$ |
| 10                                | 0.549683   $-6.02^\circ$ | 0.835374   $4.58^\circ$ |

| H-plane $f/f_c = 1.5$ |                           |                          |
|-----------------------|---------------------------|--------------------------|
| M                     | $S_{11}$                  | $S_{21}$                 |
| 1                     | 0.434026   $-85.43^\circ$ | 0.900900   $23.43^\circ$ |
| 2                     | 0.417444   $-88.59^\circ$ | 0.908703   $22.12^\circ$ |
| 3                     | 0.415904   $-89.04^\circ$ | 0.909409   $21.96^\circ$ |
| 4                     | 0.415558   $-89.19^\circ$ | 0.909567   $21.91^\circ$ |
| 5                     | 0.415456   $-89.26^\circ$ | 0.909613   $21.89^\circ$ |
| 6                     | 0.415424   $-89.30^\circ$ | 0.909628   $21.88^\circ$ |
| 7                     | 0.415418   $-89.32^\circ$ | 0.909631   $21.87^\circ$ |
| 8                     | 0.415421   $-89.34^\circ$ | 0.909629   $21.87^\circ$ |
| 9                     | 0.415427   $-89.35^\circ$ | 0.909627   $21.87^\circ$ |
| 10                    | 0.415434   $-89.36^\circ$ | 0.909623   $21.86^\circ$ |

**Table I.** Convergence of scattering parameters versus mode numbers M for E- and H-plane right angle bends.

image waveguide in  $y < 0$ . We have used the lowest nine modes in waveguides *I* and *II* for the junction in E-plane and the lowest five modes for the junction in H-plane. The same numbers of modes are used for the E-plane and H-plane problems throughout the numerical examples in the following. The scattering parameters of the symmetric E-plane T-junction with  $a = 2b = 1.7$  inch and  $d_I = d_{II} = w_I = w_{II} = 0.85$  inch are shown in Fig. 5 and compared with those obtained by the three plane mode-matching technique [10] and the measured data [10]. In Fig. 5,  $\lambda_g$  denotes the wavelength of  $TE_{10}$  mode in waveguide *I*.

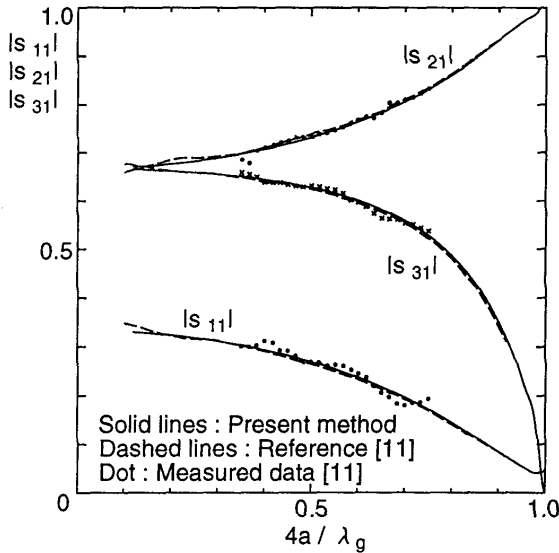


**Figure 5.** Reflection coefficient  $|S_{11}|$  as functions of frequency for E-plane right angle corner-bends with  $w_{II} = d_{II} = 0$  and  $d_I = w_I$  in Fig. 1.

Figure 6 shows the similar comparison for the symmetric H-plane T-junction with  $b = 2a = d_I = d_{II} = w_I = w_{II} = 0.45$  inch. For both the E-plane and H-plane T-junctions, the results of the present method are in close agreement with those obtained by the three plane mode-matching technique [10] and measurements [10] over the total waveguide frequency band.

Next we consider the asymmetric T-junction. The scattering parameters of the E-plane junction with  $a = 7.8995$  mm,  $b = 2.19$  mm,  $d_I = w_I = 3.95$  mm,  $d_{II} = 5.6945$  mm, and  $w_{II} = 2.205$  mm are shown in Fig. 7 as functions of frequency and compared with those obtained by the  $TE^x$  mode-matching method [9] and the method of lines [4]. The present results agree well with those of the method of lines. Some discrepancy is observed in the results of the  $TE^x$  mode-matching method. This is because the number of modes used in [9] was not sufficient for the accurate computation. Figure 8 shows the similar results for the asymmetric H-plane T-junction with  $b = 2a = d_I = w_I = 0.45$  inch and  $d_{II} = w_{II} = 0.3375$  inch. The scattering parameters change

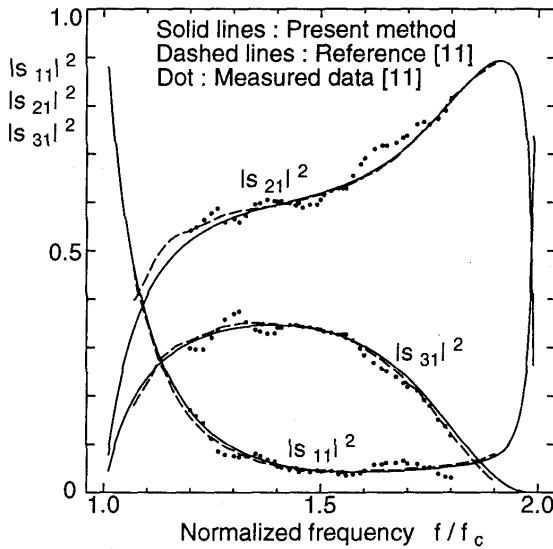
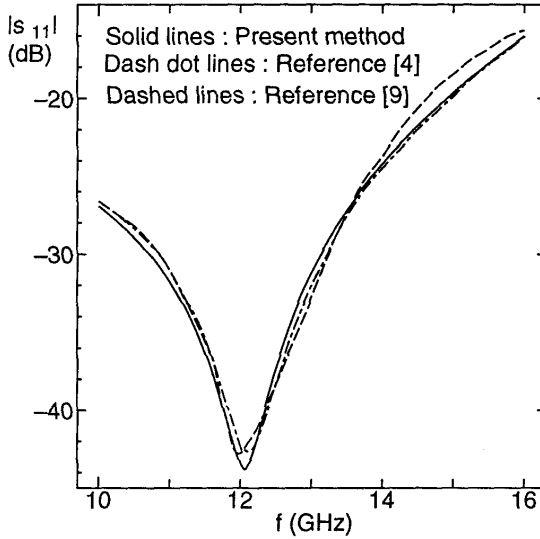


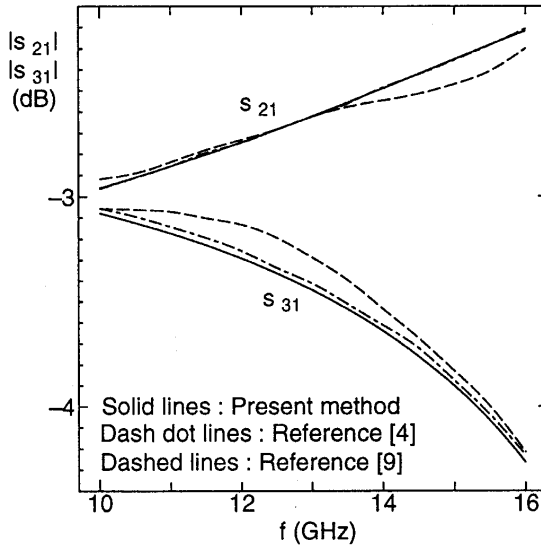
**Figure 6.** Power transmission coefficient  $|S_{21}|^2$  as a function of frequency for a H-plane right angle corner-bend.

abruptly in the frequency range  $f/f_c \leq 1.33$  where the dominant mode in waveguide *II* becomes cutoff, but otherwise their characteristics are similar to those of the symmetric T-junction shown in Fig. 6.

Finally we discuss the problem of two series E-plane T-junctions shown in Fig. 2. The scattering parameters of the series E-plane junctions with  $a = 3.556$  mm,  $b = 0.75$  mm,  $d_I = w_I = 1.778$  mm,  $d'_I = w'_I = w_{II} = 1.27$  mm,  $d_{II} = 2.286$  mm,  $b' = 0.805$  mm,  $d'_{II} = 1.91$  mm,  $w'_{II} = 0.63$  mm, and  $l = 5.12$  mm are shown in Fig. 9 and compared with those obtained by the  $TE^x$  mode-matching method [9]. We can see that both results show similar features as functions of frequency. The results of the  $TE^x$  mode-matching method [9] include some errors, since the number of modes used in the modal expansion was not sufficient. The discrepancy with the present accurate analysis is less than about 4% for the two series case.



(a)



(b)

**Figure 7.** Scattering parameters as functions of frequency for an asymmetric E-plane T-junction with  $a = 7.8995$  mm,  $b = 2.19$  mm,  $d_I = w_I = 3.95$  mm,  $d_{II} = 5.6945$  mm, and  $w_{II} = 2.205$  mm.

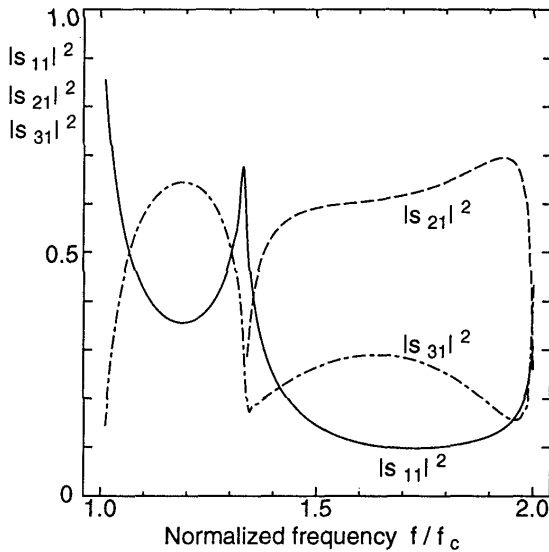
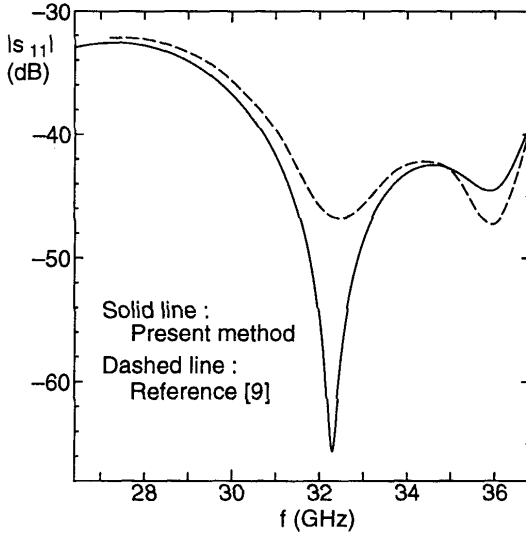


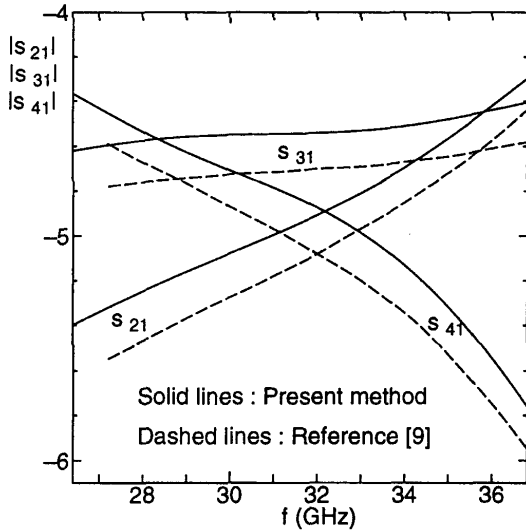
**Figure 8.** Scattering parameters as functions of frequency for an asymmetric H-plane T-junction with  $b = 2a = d_I = w_I = 0.45$  inch and  $d_{II} = w_{II} = 0.3375$  inch.

#### 4. CONCLUSION

A rigorous and efficient method for the analysis of rectangular waveguide junctions has been presented. The method is a combination of the Fourier transform technique and mode-matching. By introducing an image waveguide to the side-arm of a junction, the problem of waveguide junction has been reduced to a simpler aperture problem in a uniform rectangular waveguide to which the Fourier transform technique can be applied. The fields in the cavity region expressed by the Fourier integrals are evaluated in closed form by a simple residue-calculus. This reduces significantly the number of unknowns for characterizing the waveguide junction. The scattering parameters can be calculated by solving matrix equations of relatively small dimensions. The numerical results for right-angle corner bends, symmetric E- and H-plane T-junctions, asymmetric E- and H-plane T-junctions, and asymmetric series E-plane T-junctions agree very well with literatures.



(a)



(b)

**Figure 9.** Scattering parameters as functions of frequency for the asymmetric series E-plane T-junctions shown in Fig. 2. Waveguide dimensions:  $a = 3.556$  mm,  $b = 0.75$  mm,  $d_I = w_I = 1.778$  mm,  $d'_I = w'_I = w_{II} = 1.27$  mm,  $d_{II} = 2.286$  mm,  $b' = 0.805$  mm,  $d'_{II} = 1.91$  mm,  $w'_{II} = 0.63$  mm, and  $l = 5.12$  mm.

## REFERENCES

1. Koshiba, M., M. Sato, and M. Suzuki, "Application of finite-element method to H-plane waveguide discontinuities," *Electron. Lett.*, Vol. 18, 364–365, 1982.
2. Koshiba, M., and M. Suzuki, "Application of the boundary-element method to waveguide discontinuities," *IEEE Trans. Microwave Theory Tech.*, Vol. 34, 301–307, 1986.
3. Pascher, W., and R. Pregla, "Analysis of rectangular waveguide discontinuities by the method of lines," *IEEE Trans. Microwave Theory Tech.*, Vol. 43, 416–420, 1995.
4. Pascher, W., and R. Pregla, "Analysis of rectangular waveguide junctions by the method of lines," *IEEE Trans. Microwave Theory Tech.*, Vol. 43, 2649–2653, 1995.
5. Alessandri, F., M. Mongiardo and R. Sorrentino, "Computer-aided design of beam forming networks for modern satellite antennas," *IEEE Trans. Microwave Theory Tech.*, Vol. 40, 1117–1127, 1992.
6. Alessandri, F., M. Mongiardo, and R. Sorrentino, "Rigorous mode matching analysis of mitered E-plane bends in rectangular waveguide," *IEEE Microwave and Guide Wave Lett.*, Vol. 4, 408–410, 1994.
7. Alessandri, F., M. Mongiardo, and R. Sorrentino, "A technique for the fullwave automatic synthesis of waveguide components: application to fixed phase shifters," *IEEE Trans. Microwave Theory Tech.*, Vol. 40, 1484–1495, 1992.
8. Kühn, E., "A mode-matching method for solving field problem in waveguide and resonator circuits," *Arch. Elek. Übertragung*, Vol. 27, 511–518, 1973.
9. Arndt, F., I. Ahrens, U. Papziner, U. Wiechmann, and R. Wilkeit, "Optimized E-plane T-junction series power dividers," *IEEE Trans. Microwave Theory Tech.*, Vol. 35, 1052–1059, 1987.
10. Sieverding, T., and F. Arndt, "Field theoretic CAD of open or aperture matched T-junction coupled rectangular waveguide structures," *IEEE Trans. Microwave Theory Tech.*, Vol. 40, 353–362, 1992.
11. Liang, X., K. A. Zaki, and A. E. Atia, "Rigorous three plane mode-matching technique for characterizing waveguide T-junctions, and its application in multiplexer design," *IEEE Trans. Microwave Theory Tech.*, Vol. 39, 2138–2147, 1991.
12. Ma, Z., and E. Yamashita, "Port reflection coefficient method for solving multi-port microwave network problems," *IEEE Trans. Microwave Theory Tech.*, Vol. 43, 331–337, 1995.

13. Rebollar, J. M., J. Esteban, and J. E. Page, "Fullwave analysis of three and four-port rectangular waveguide junctions," *IEEE Trans. Microwave Theory Tech.*, Vol. 42, 256–263, 1994.
14. Lewin, L., *Theory of Waveguides*, Chapter 8, London: Newnes-Butterworths, 1975.
15. Lee, J. H., H. J. Eom, J. W. Lee, and K. Yoshitomi, "Transverse electric mode scattering from rectangular grooves in parallel plate," *Radio Science*, Vol. 29, 1215–1218, 1994.
16. Lee, J. W., and H. J. Eom, "TE-mode scattering from two junctions in H-plane waveguide," *IEEE Trans. Microwave Theory Tech.*, Vol. 42, 601–606, 1994.
17. Iatrou, C. T., and M. Cavenago, "Field analysis of rectangular waveguide open junction," *IEEE Trans. Microwave Theory Tech.*, Vol. 45, 165–172, 1997.